Sensitivity of Simulated Nocturnal Convective Systems to Graupel Sedimentation Characteristics

Frederick Iat-Hin Tam, Ming-Jen Yang

National Taiwan University,

Taipei, Taiwan

Abstract

In this study, results from different microphysical sensitivity experiments on a Great Plains nocturnal convective system was presented to show a sensitivity between vital system thermodynamical and kinematic structures to various assumptions in graupel sedimentation characteristics in a two-moment microphysical scheme.

The results suggest that system updrafts will be stronger and have a greater tendency to concentrate near the system edge when graupel hydrometeors are allowed to sediment at different rates in accordance with their size (size sorting). In these experiments, preferential melting of heavier graupel below updrafts sharpens the buoyancy gradient there, which horizontally expands and strengthens the system rear-inflow jet (RIJ). This could positively impact the overall updraft strength by releasing more latent heat via riming and vapor deposition as graupel hydrometeors are re-transported back to the updrafts by the stronger RIJ.

Key word: Precipitation Process; Cloud Microphysics; Mesoscale Dynamics

1. Introduction

A substantial part of the errors in convective scale quantitative precipitation forecast (QPF) could be attributed to inaccurate hydrometeor drop size distribution (DSD) within convective systems, especially for simulations where bulk microphysical schemes are used (Milbrandt and McTaggart-Cowan 2010). There are two possible explanations for such inaccuracies: Firstly, they often utilize prescribed gamma DSD (Seifert and Beheng 2006), which often deviate from in-situ observations (Adirosi et al. 2014). Secondly, bias in various hydrometeor sedimentation characteristics could limit the ability for models to accurately represent DSD variabilities in convective systems.

Past studies have indicated that storm intensity, longevity, and accumulated precipitation to be heavily impacted by rimed particle sedimentation characteristics aloft (Yang and Houze 1995; van den Heever and Cotton 2004; Adams-Selin et al. 2013). It is well known that updraft intensity is sensitive to the vorticity balance between cold pool and environmental shear (Rotunno et al. 1988), with the strongest updrafts occurring when a balance state is reached between the two vorticity sources. Thus, it is possible that the sensitivities to sedimentation could be interpreted through cold pool dynamics. Substantial uncertainties exist with this hypothesis, however. For example, recent studies (van den Heever and Cotton 2004; Adams-Selin et al. 2013) indicated increased rimed particle density to be a hinderance to the overall system strength due to slower cold pool accumulation. Other studies, such as van Weverberg et al. (2012), shows a contradictory result where heavier rimed particles are linked to stronger cold pools instead.

Apart from cold pools, another feature that is impacted by these differences seem to be the system's rear inflow. Adams-Selin (2013) shows more elevated rear inflows for experiments with greater rimed particle density. Elevated rear inflows could be beneficial to mid-level updraft intensification either by neutralizing the environmental vorticity aloft or by releasing extra latent heat through riming (Siegel and van den Heever 2013).

The above discussion shows that the responses to rimed particle characteristics are complex and controlled by multiple competing factors. A further complication is that past studies generally utilize single moment microphysical schemes, which cannot reproduce hydrometeor size sorting. The lack of size sorting might be of relevance in determining the DSD distribution near updraft, especially when accompanied with the system's internal circulation. For example, size sorting for hail particles was shown to be critical in creating Z_{DR} arcs in supercell storms since heavier particles could then sediment at locations closer to the updrafts than lighter particles (Dawson et al. 2013).

While the role of rimed particle sedimentation in DSD adjustment have been established for supercells, the effect of these DSD changes of the system's kinematic and thermodynamical structures has been relatively unexplored. There is also a lack of modeling studies on non-supercellular systems, including squall lines. These considerations motivate our current study, where the kinematic and thermodynamical responses of a nocturnal

squall line to sedimentation characteristics are explored through a set of microphysical sensitivity experiments.

2. Description of microphysical sensitivity experiments

We performed a series of simulations with Version 3.9 of the WRF-ARW model on a Great Plains nocturnal squall line system on 15 July 2015. To ensure consistency, all simulations in this study utilize the two-moment version of the National Severe Storms Laboratory (NSSL) scheme. Results of the following set of simulations would be discussed in detail in this extended abstract.

Sensitivity experiments on size sorting

This set of experiments include three simulations: GNSS, RNSS, and GRNSS. These acronyms represent disabling graupel size sorting, disabling rainwater size sorting, and disabling both graupel and rainwater size sorting, respectively. Disabling size sorting for a specific hydrometeor category could be accomplished by letting the corresponding hydrometeor mixing ratio and number concentration to sediment under the same terminal velocity.

3. Results and Discussions

3.1. Structural comparison on simulated systems

Figure 1 compares the line-averaged reflectivity cross section for size sorting simulations during their respective mature phases. We first notice that by disabling graupel size sorting, the overall line-averaged system structure transitioned from a clear leading line-trailing stratiform structure to a structure that is dominated by its stratiform region (Fig.1b,d). Contrastingly, disabling the rainwater size sorting seems to have little impact on the simulated system, as shown by the structural similarities between the FULL (Fig.1a) and the RNSS (Fig.1c). This suggests that hydrometeor size sorting for rimed particles would initiate a more permanent change on the overall system structure, while rainwater size sorting likely induces a more transient response.

We further note that the lack of a well-defined convective region in the GNSS and GRNSS could point to weaker updrafts, especially near the system edge. This could also indicate differences in storm circulation between experiments.

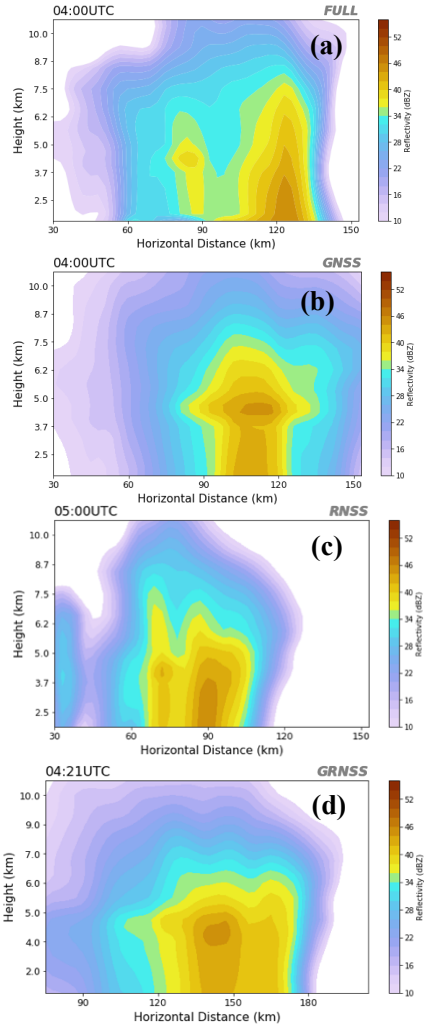

Figure 1 Line-averaged reflectivity cross sections for (a) FULL, (b) GNSS, (c) RNSS, and (d) GRNSS.

3.2. Statistical analysis on system updraft strength

Results from Section 3.1 points to potentially weaker convective updrafts when rimed particle size sorting was turned off. Updraft statistics during the simulated systems' developing, mature and weakening phases (Fig.2) are generally consistent with the above assessment, with the FULL (and RNSS) featuring greater tendency for stronger updrafts during mature phase than the other two experiments. This comparison indicates that graupel size sorting might decelerates the updraft weakening rate as cold pool accumulates (which would weaken the updrafts through enhanced tilt).

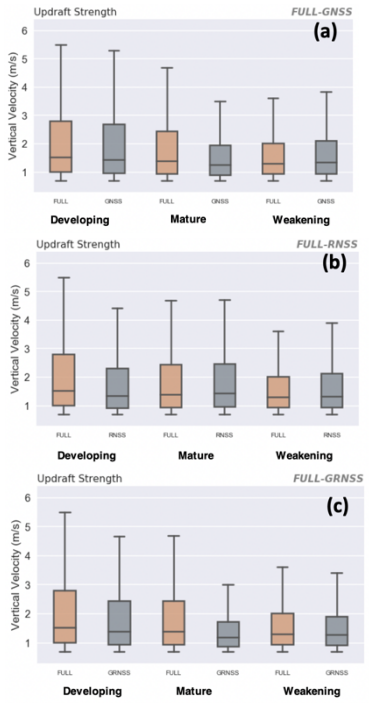

Figure 2 Box-and-whisker plots for (a) FULL (Brown) and GNSS (Gray) during developing, mature and weakening phases. (b) Same as (a), but for RNSS (Gray). (c) Same as (a), but for GRNSS (Gray).

Next, mature phase CFADs (Contoured Frequency by Altitude Diagrams) for the GNSS and RNSS are compared to the FULL are compared in Figure 3 in an attempt to understand whether the differences in Figure 2 are dominated by low-level updrafts or by mid-level updrafts. For the GNSS (Fig.3a), there is a greater possibility for stronger updrafts to occur ***above*** *the melting level* for the FULL while the updraft statistics were similar below the melting level (as shown by the 0.135 frequency contour[1]). As low-level updrafts are often mechanically forced by cold pools, it is possible that cold pool dynamics alone is not sufficient in causing the updraft differences between the two experiments. For the RNSS, the mid-level updrafts are similar to in strength to the FULL while slightly weaker than the FULL below the melting level. This result reiterates the dominant role of mid-level updrafts on the overall updraft statistics.

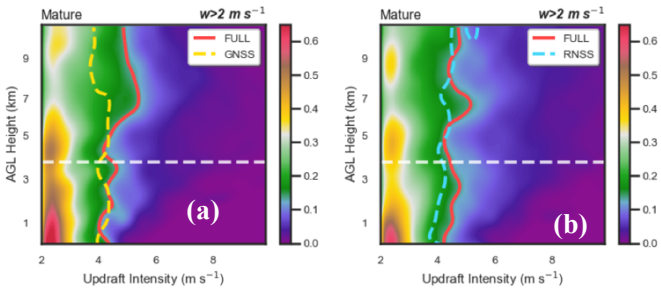

[1] This value was chosen since it encompassed the updrafts strength bracket of 4.5-5 m s^{-1}, where the greatest difference between the FULL and GNSS occurred (Fig. 2)

Figure 3 (a) Strong updrafts (w>2 ms^{-1}) CFADs during the mature phase, the 0.135 frequency contours for the FULL (red solid) and the GNSS (yellow dashed) are shown. (b) Same as (a), but for RNSS (blue dashed). White dashed lines represent the approximate height for the 0 ºC level. For reference, the FULL CFAD is shown as filled contours.

3.3. Potential explanation of mid-level updraft intensification in the FULL

We will now try to examine the factors that inhibited updraft intensification when graupel size sorting was disabled (GNSS). First, the line-averaged buoyancy cross section (Fig.4) showed sharper buoyancy gradient near the convective updrafts as both the positive buoyancy above the melting level and the negative buoyancy below the melting level are stronger than in the GNSS. The line-averaged storm circulations in Figure 4 also suggest that the rear inflow will be weaker and less horizontally expanded if graupel size sorting was turned off. This suggests that, similar to Siegel and van den Heever (2013), the origin of the updraft strength differences between the FULL and GNSS might be the extra latent heat release when graupel was re-entrained into the updrafts by the rear inflow.

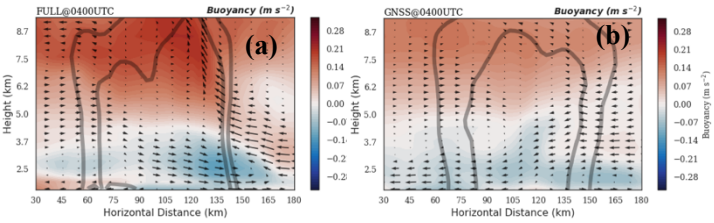

Figure 4 (a) Line-averaged cross section of FULL buoyancy (m s^{-2}; shading), 20 and 30 dBZ outline (thick gray contours) and storm-relative wind (vectors) at 0400UTC. (b) Same as (a), but for GNSS at 0400UTC.

To account for this, we further examine the joint distribution of graupel number concentration (N_g) and air temperature for the FULL, GNSS, and RNSS (Fig.5). The graupel distributions for the FULL and RNSS are similar for most temperature values (Fig.5b). The GNSS, however, features substantially less graupel below 0ºC. Graupel underproduction for the GNSS is especially prominent in the temperature range between -3ºC and -10ºC. Enhanced graupel production at this temperature range is consistent with increased riming process, the excess heat release of which could well potentially increased the positive buoyancy, and in turn, strengthens the mid-level updrafts. Furthermore, we notice that more graupel existed below the melting level in the FULL than the GNSS. The melting of these excess graupel would then further increase the buoyancy gradient near system edge. Finally, the joint distributions were similar between

the RNSS and the FULL, which agrees with our prior findings that mixed phase particle size sorting was more vital than rainwater size sorting in adjusting the systems' strength.

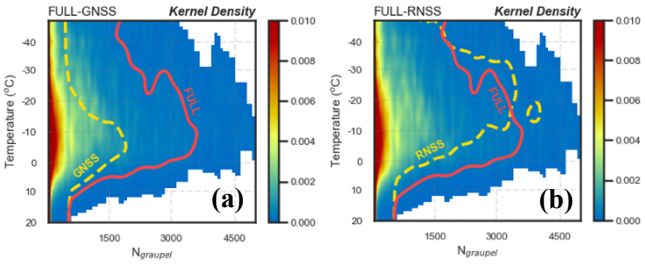

Figure 5 Joint distribution of graupel number concentration and air temperature during system mature phase. (a) compares the kernel density 0.025 contours for the FULL (red) and GNSS (yellow), whereas (b) compares the FULL (red) and the RNSS (yellow). In both plots, the FULL distribution was shaded for reference.

3.4. RIJ strengthening for systems with graupel size sorting: A Dynamical Analysis

Through the above analyses, a clearer picture emerges as to why the mid-level updrafts tend to be stronger when graupel size sorting exists. It seems that the mid-level updrafts are stronger in the FULL and RNSS due to (i) excess riming as graupel re-entrained into the updrafts by the rear inflow, and (ii) melting of heavier graupel near system edge due to size sorting.

The relationship between enhanced buoyancy gradient and rear inflow intensification could be interpreted under the following dynamical framework.

$$\frac{1}{\rho_0}\nabla^2 P = -\nabla \cdot (V \cdot \nabla \mathrm{V}) + \frac{\partial B}{\partial z} \quad (Eq.1)$$

The first (second) term of the right-hand side of Equation 1 represents the dynamical and thermodynamical contributions to the pressure perturbation field, respectively. After solving the above Poisson Equation with suitable boundary conditions, we can then derive the pressure gradient force associated with ***buoyancy-induced*** (PGF_{Pb}) and ***dynamically-induced*** pressure perturbations (PGF_{Pd}).

The change rates of line-averaged wind speed associated with PGF_{Pb} are shown in Figure 6. For the FULL, rear-to-front forcing could be identified immediately behind the system edge for the FULL while the distance between the rear-to-front forcing and the system edge was substantially larger for the GNSS. Thus, we conclude that graupel size sorting is beneficial of rear inflow intensification, which has a positive impact on updraft intensity through extra latent heat release.

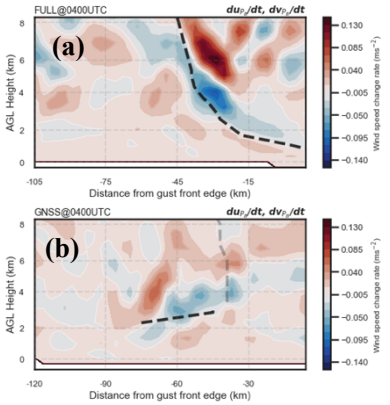

Figure 6 (a) Line-averaged cross section of the line-averaged, system-normal component of the wind speed change rate induced by the PGF_{Pb} for the FULL (shading, m s^{-2}) at 0400 UTC. Black dashed line denoted the approximate location of the convective updraft axis. (b) Same as (a), but for the GNSS at 0400 UTC. Gray dashed line denoted the updraft axis, while the black dashed line represented the descending inflow layer.

4. Summary

In this study, an attempt was made to find the thermodynamical and kinematic responses of simulated squall lines to rimed particle (graupel) sedimentation settings in microphysical schemes. Our current findings are briefly summarized in this section.

The comparison of microphysical sensitivity experiments indicates a tendency for stronger ***mid-level*** updrafts when graupel size sorting was permitted in our chosen microphysical scheme. Low-level updrafts, on the other hand, is less sensitive to graupel size sorting.

It is shown that the intensification of mid-level updrafts is intrinsically related to the strengthening and expansion of rear inflow. In a scenario where graupel size sorting exists, melting of heavier graupel particles near the system edge sharpens the buoyancy gradient, which resulted in stronger rear-to-front inflow, more efficient riming process, and stronger mid-level updrafts. If graupel size sorting is disabled, however, graupel sedimentation location shifted to the system's rear, thus substantially inhibited the expansion of the rear inflow.

5. References

Adams-Selin, R.D., S.C. van den Heever, and R.H. Johnson, 2013: Impact of Graupel Parameterization Schemes on Idealized Bow Echo Simulations. *Mon. Wea. Rev.*, **141**, 1241–1262.

Adirosi, E., E. Gorgucci, L. Baldini, and A. Tokay, 2014: Evaluation of Gamma Raindrop Size Distribution Assumption through Comparison of Rain Rates of

Measured and Radar-Equivalent Gamma DSD. *J. Appl. Meteor. Climatol*., **53**, 1618–1635.

Dawson, D.T., E.R. Mansell, Y. Jung, L.J. Wicker, M.R. Kumjian, and M. Xue, 2014: Low-Level ZDR Signatures in Supercell Forward Flanks: The Role of Size Sorting and Melting of Hail. *J. Atmos. Sci*., **71**, 276–299.

Mansell, E.R., 2010: On Sedimentation and Advection in Multimoment Bulk Microphysics. *J. Atmos. Sci.,* **67**, 3084–3094.

Milbrandt, J.A. and R. McTaggart-Cowan, 2010: Sedimentation-Induced Errors in Bulk Microphysics Schemes. *J. Atmos. Sci.,* **67**, 3931–3948.

Rotunno, R., J.B. Klemp, and M.L. Weisman, 1988: A Theory for Strong, Long-Lived Squall Lines. *J. Atmos. Sci.*, **45**, 463–485.

Seigel, R.B. and S.C. van den Heever, 2013: Squall-Line Intensification via Hydrometeor Recirculation. *J. Atmos. Sci.*, **70,** 2012–2031.

Seifert, A., and K. D. Beheng, 2006: A two-moment cloud microphysics parameterization for mixed-phase clouds. Part I: Model description. *Meteor. Atmos. Phys.*, **92**, 45–66.

van den Heever, S. C., and W. R. Cotton, 2004: The impact of hail size on simulated supercell storms. *J. Atmos. Sci.*, **61**, 1596–1609.

van Weverberg, K., A. M. Vogelmann, H. Morrison, and J. Milbrandt, 2012: Sensitivity of idealized squall-line simulations to the level of complexity used in two-moment bulk microphysics schemes. *Mon. Wea. Rev.,* **140**, 1883–1907.

Yang, M. J., and R. A. Houze Jr., 1995: Sensitivity of squall-line rear inflow to ice microphysics and environmental humidity. *Mon. Wea. Rev.,* **123**, 3175–3193.

6. Acknowledgement

This work was supported by the Ministry of Science and Technology of Taiwan under Grant MOST- 106-2111-M-002-004. The authors are grateful to Dr. Wen-Chau Lee (NCAR) for continued support and guidance.